

Flux Cancellation Rates and Converging Speeds of Cancelling Magnetic Features

Jongchul Chae^{1,2}, Yong-Jae Moon^{2,3}, Haimin Wang² and H. S. Yun⁴

¹*Department of Astronomy and Space Science, Chungnam National University, Daejeon 305-764, Korea; chae@cnu.ac.kr*

²*Big Bear Solar Observatory, New Jersey Institute of Technology, 40386 North Shore Lane, Big Bear City, CA 92314, U.S.A.*

³*Korea Astronomy Observatory, Yooseong, Daejeon 305-348, Korea*

⁴*Astronomy Program, SEES, Seoul National University, Seoul 151-742, Korea*

Draft on October 4, 2001

Abstract. Cancelling magnetic features are commonly believed to result from magnetic reconnection in the low atmosphere. According to the Sweet-Parker type reconnection model, the rate of flux cancellation in a cancelling magnetic feature is related to the converging speed of each pole. To test this prediction observationally, we have analyzed the time-variation of two cancelling magnetic features in detail using the high-resolution magnetograms taken by the Michelson Doppler Imager (MDI) on the Solar and Heliospheric Observatory (SOHO). As a result, we have obtained the rate and converging speed of flux cancellation in each feature: 1.3×10^{18} Mx h⁻¹ (or 1.1×10^6 G cm s⁻¹ per unit contact length) and 0.35 km s⁻¹, in the smaller one, and 3.5×10^{18} Mx h⁻¹ (1.2×10^6 G cm s⁻¹) and 0.27 km s⁻¹ in the bigger one. The observed speeds are found to be significantly bigger than the theoretically expected ones, but this discrepancy can be resolved if uncertainty factors such as low area filling factor of magnetic flux and low electric conductivity are taken into account.

1. INTRODUCTION

Magnetic fluxes of opposite polarities often collide and cancel on the solar surface (Martin et al., 1985; Livi et al., 1985). Flux cancellation appears to play an important role in various kinds of dynamic activities in the upper atmosphere of the Sun, as seen from its observed associations with flares (Livi et al., 1989; Wang and Shi, 1993) microflares/surges/jets (Chae et al., 1999), X-ray bright points (Webb et al., 1993), erupting mini-filaments (Hermans and Martin, 1986), transition region explosive events (Dere et al., 1991; 1991; Chae et al., 1998), filament formation (Martin, 1986; Chae et al., 2000, 2001), filament activation and eruption (Wang et al., 1996; Kim et al., 2001), and coronal mass ejections (Zhang et al., 2001)).

Observations support that flux cancellation may be a result of submergence of magnetic field lines following magnetic reconnection that occurs in the low atmosphere of the Sun. The evidence that magnetic



© 2001 Kluwer Academic Publishers. Printed in the Netherlands.

flux retracts below the surface during flux cancellation came from the comparisons of photospheric magnetograms and chromospheric magnetograms done by Harvey et al. (1999). Moreover, the observational studies of field-line connectivity (Martin, 1990; Wang and Shi, 1993) have indicated that magnetic poles involved in flux cancellation are not connected to each other initially. These observations are consistent with the picture of reconnection-and-submergence of initially unconnected field lines.

Recently, magnetic reconnection in the photosphere and chromosphere was theoretically described either using Sweet-Parker type quasi-state reconnection current sheet (Litvinenko, 1999) or based on the time-dependent tearing mode instability (Sturrock, 1999). Litvinenko's model is of specific interest to us since it provides a way of linking observed parameters of cancelling magnetic features to physical parameters of reconnection current sheet. There are two observational parameters that are important in Litvinenko's model: the rate of flux cancellation and the inflow speed. Litvinenko and Martin (1999) determined these parameters in a cancelling magnetic feature in an active region and they found a fairly good agreement between the observed parameters and theoretical values. This work has motivated our study.

The objective of the present paper is to understand further the properties of low-atmosphere reconnection using detailed observations of cancelling magnetic features. Specifically we are going to determine the rates of flux cancellation and converging speeds in two cancelling magnetic features by carefully examining the time-sequence of magnetograms. We will discuss the implications of the observed parameters based on Litvinenko's model.

2. DATA ANALYSIS

We use high-cadence, high-resolution magnetograms taken by the Michelson Doppler Imager (MDI) on board the Solar and Heliospheric Observatory. We first aligned one-minute cadence magnetograms by taking into account the solar differential rotation and then averaged five frames to produce high signal-to-noise ratio. A comparison of two successive 5-min averaged magnetograms indicates that the root-means-square level of noise is about 3.5 G per pixel.

The magnetogram data covered a small active region NOAA 8011 that was located near disk center. The active region was slowly decaying at the time of observations. Many cancelling magnetic features were found in this active region, but here we study in detail only two representative features 1) that are well separated from other magnetic

elements, 2) that have positive and negative fluxes roughly balanced to each other, and 3) that have life-times longer than a couple of hours.

We determine the magnetic flux and central position of the positive polarity as functions of time using the formulae

$$\Phi_+ = \int_P B_z dS \quad (1)$$

$$(x_+, y_+) = \frac{\int_P (x, y) B_z dS}{\Phi_+} \quad (2)$$

with the integrations being performed over the pixels of positive flux density inside a small region surrounding the colliding bipole. Following the same way, the magnetic flux Φ_- and central position (x_-, y_-) of the negative polarity are determined by performing the integrations over the pixels of negative flux density inside the same region of interest. Then, the separation s between the two poles is given by

$$s = \sqrt{(x_+ - x_-)^2 + (y_+ - y_-)^2} \quad (3)$$

and the approaching speed of each polarity toward the polarity reversal boundary, by

$$v_{\text{app}} = -\frac{1}{2} \frac{ds}{dt}. \quad (4)$$

Finally, the spatial extent of the magnetic flux of positive polarity along the interface between the two polarities is determined from the expression

$$L_+ = 2.35 \sqrt{\frac{\int [(x - x_+)(y_+ - y_-)/s - (y - y_+)(x_+ - x_-)/s]^2 B_z dS}{\Phi_+}} \quad (5)$$

Here the numeric factor 2.35 is to obtain the full width at half maximum from the standard deviation assuming the spatial distribution of magnetic flux is Gaussian. The spatial extent of negative flux L_- can be obtained in the same way. In the case of the events selected in the present study, L_+ and L_- are about the same. If they differ much, the smaller value should be adopted for the spatial extent of flux cancellation site L .

3. RESULTS

3.1. CASE A

Figure 1 shows the evolution of a typical cancelling magnetic feature. It consists of two magnetic flux patches of opposite polarities approaching

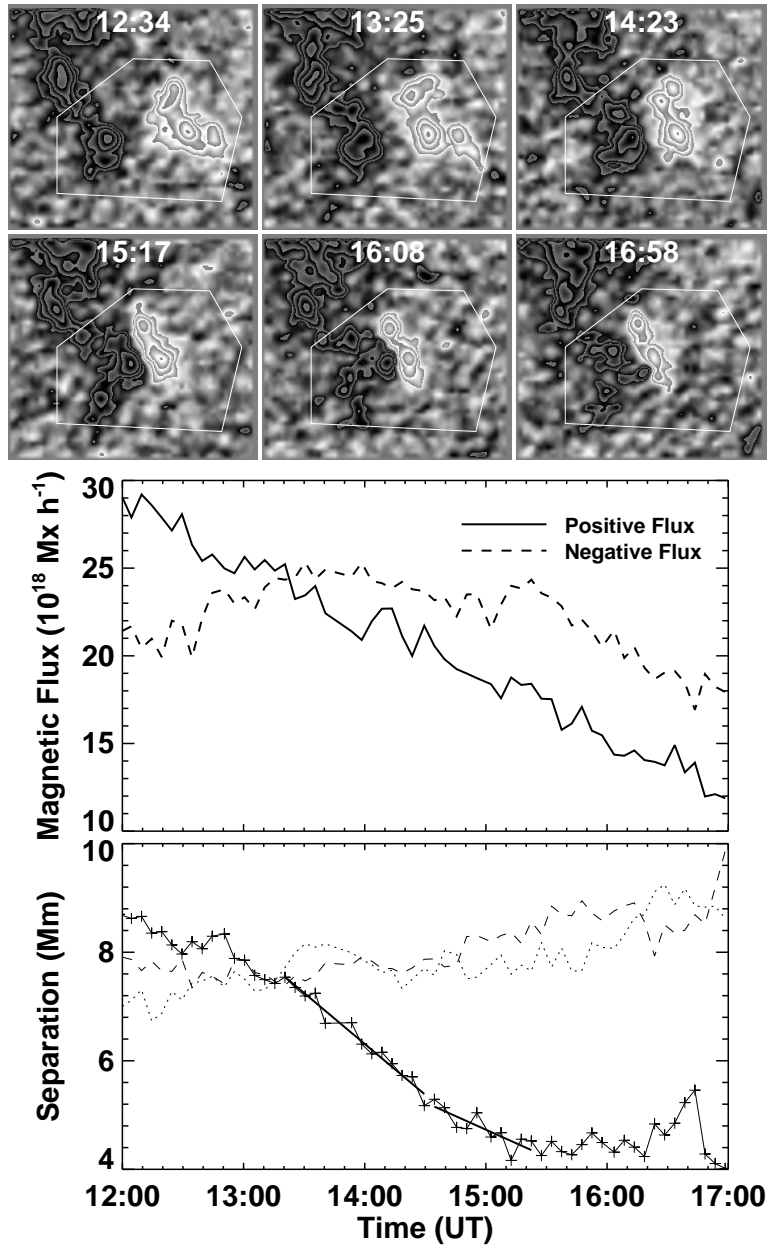


Figure 1. *Top:* a time-sequence of magnetograms showing the temporal variation of magnetic fluxes in a region A of $34'' \times 34''$ or 25000 km by 25000 km. Shown in gray-scale discontinuities are flux densities of $\pm 20, 40, 80$ G and so on. The polygon denotes the boundary of the area in which the integration of magnetic fluxes is done. *Middle:* the time-variation of the integrated magnetic fluxes Φ_+ and Φ_- . *Bottom:* the separated distance s (solid curve) and the contact lengths L_+ (dotted curve) and L_- (dashed curve)

each other. The positive polarity flux was initially about 2.9×10^{19} Mx, and steadily decreased at a nearly constant rate of 3.4×10^{18} Mx h^{-1} . Since the spatial extent of the flux cancellation interface is about $L = 7.8$ Mm, the rate of flux cancellation per unit length, which we may call the specific rate of flux cancellation, becomes 0.44×10^{18} Mx h^{-1} Mm^{-1} or 1.2×10^6 G cm s^{-1} .

The negative polarity shows a different pattern of flux evolution: its magnetic flux initially increased, stayed constant, and then decreased. This complex pattern of negative flux evolution may be a result of the combined effect of the cancellation of the flux inside the region of interest and the inflow of magnetic flux across the boundary.

The lower panel of Figure 1 shows the separation between the two polarities as a function of time. It is seen from the plot that the approaching speed *apparently* slowed down with time. The approaching speed $v_{\text{app}} \equiv -0.5ds/dt$ was about 0.27 km s^{-1} between 13:30 UT and 14:30 UT, but decreased to its half value 0.14 km s^{-1} between 14:30 UT and 15:30 UT, and was close to zero after then. Later in this section, we will show that this kind of apparent slow-down may not be real.

3.2. CASE B

Figure 2 shows another example of a cancelling magnetic feature. The positive polarity initially had small magnetic flux of about 2.5×10^{18} Mx, one order-of-magnitude smaller than in Case A. Around 00:30 UT, its flux began to decrease at a rate of 1.3×10^{18} Mx h^{-1} . The length of the flux cancellation interface was about 3.3 Mm, so the specific rate of flux cancellation is estimated to be about 0.40×10^{18} Mx h^{-1} Mm^{-1} or 1.1×10^6 G cm s^{-1} . Interestingly this value is very close to the one in the bigger cancelling magnetic feature A. We, however, can not tell whether this match is just a coincidence or it may indicate a possible constancy of specific flux cancellation rate. Statistical studies based on a number of events will be required to determine whether the observed close match of specific flux cancellation rate is physically significant or not.

The positive flux patch and negative flux patch initially stayed without approaching motion for a while. Around 00:30 UT, they suddenly began to move to each other at a speed of 0.35 km s^{-1} . Then, the approaching speed decreased to its half value 0.22 km s^{-1} (1:20 to 2:20 UT), and eventually became zero. This slow-down of the approaching speed in case B is qualitatively similar to the behavior of flux motion in case A. The major difference is in the value of the initial speed. The smaller feature B had a higher value of 0.35 km s^{-1} than the bigger feature A with 0.27 km s^{-1} .

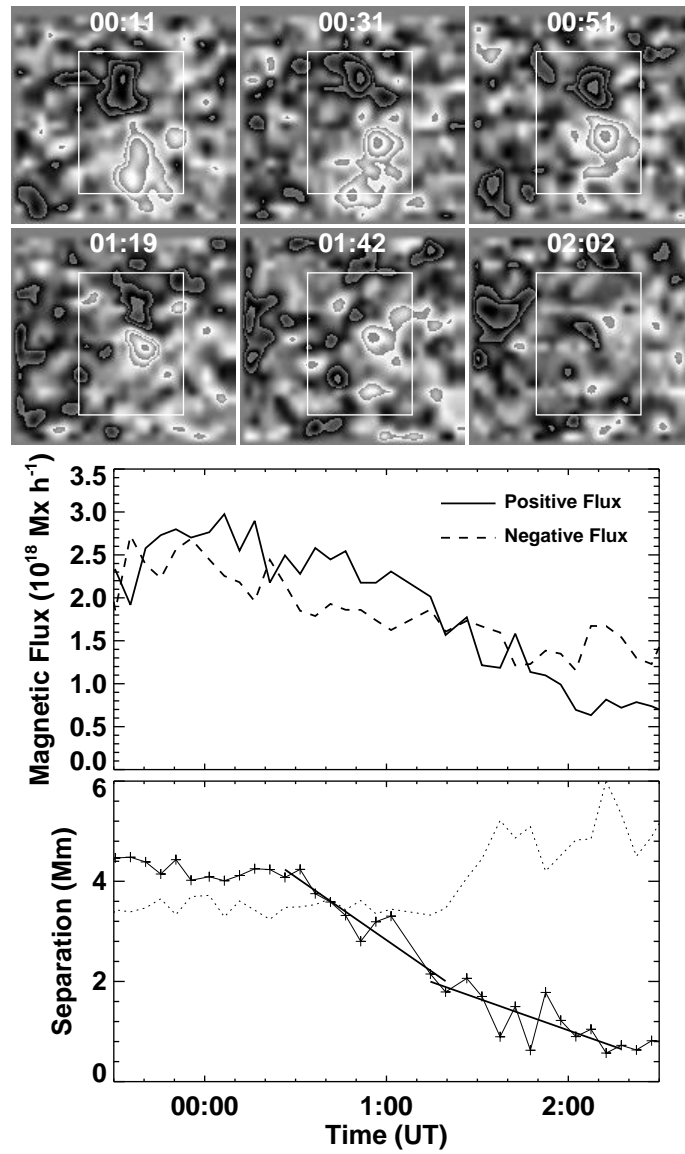


Figure 2. The same as in Figure 1, but for a smaller region B of $18'' \times 18''$ or 13000 km by 13000 km. The lowest gray-scale discontinuity in the top panel here represents ± 10 G.

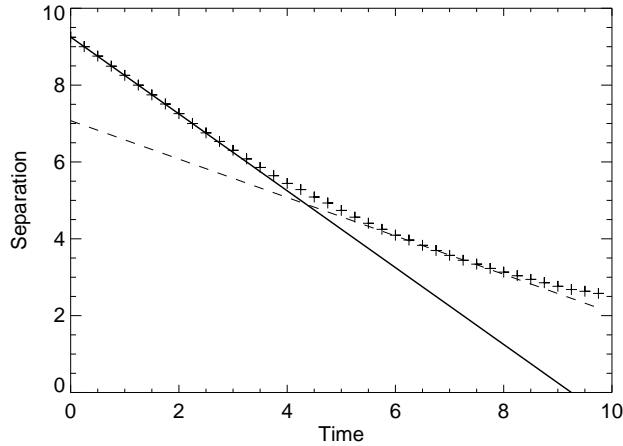


Figure 3. The separation between the centers of two hypothetical poles that move at a constant speed toward the interface of flux cancellation (+ symbols). The solid line describes the early phase before they come into close contact, while the dashed line describes the phase during the close contact. The slope of the dashed line (i.e., apparent speed) is half of that of the solid line (that is equal to the true speed).

3.3. INTERPRETATION OF THE SLOWING-DOWN OF THE APPROACH

A caution should be made in interpreting the observed slowing-down of the approaching speed between the positive and negative flux patches. When the two flux patches are away from each other and are not in a close contact, the observed approaching speed is the same as the speed of flux transport. As soon as they come into a close contact and, as a result, fluxes of opposite polarities begin to cancel, the approaching speed apparently slows down. The reason is that the head part of the flux patch moving toward the cancellation interface disappears when it reaches the interface, and the interface remains stationary without moving whereas the tail part of the flux patch is still observed to be moving toward the interface. As a result, the center of the flux patch appears to be moving at a speed significantly smaller than the true speed of flux transport, most likely at half of the true speed during the major phase of flux cancellation.

To support our interpretation of the observed slowing-down of the approaching speed of the flux patches, we use a simple model of two hypothetical poles of opposite polarities that approach toward the interface of flux cancellation at a constant speed. Figure 3 shows the separation of the two poles as a function of time. The separation has been determined from the flux-weighted centers of the two flux patches as in the case of the observed cancelling magnetic features. It is shown in

Table I. Observed parameters of cancelling magnetic features.

Parameter	Case A	Case B
Initial magnetic flux Φ_0	2.9×10^{19} Mx	2.5×10^{18} Mx
Flux cancellation rate $\frac{d\Phi}{dt}$	3.4×10^{18} Mx h ⁻¹	1.3×10^{18} Mx h ⁻¹
Contact length L	7.8 Mm	3.3 Mm
Specific cancellation rate $r_{obs} = \frac{d\Phi/dt}{L}$	1.2×10^6 G cm s ⁻¹	1.1×10^6 G cm s ⁻¹
Converging speed v_c	0.27 km s ⁻¹	0.35 km s ⁻¹

Figure 3 that the approaching speed of the two poles apparently slows down like the observed ones shown in Figures 1 and 2 even if they move at a constant speed. Therefore, we conclude that the observed slowing-down of the approaching speed is not real, and is not incompatible with the constant speed of magnetic flux transport toward the interface of flux cancellation.

3.4. COMPARISON WITH PREVIOUS MEASUREMENTS

Table I summarizes our observation. Even though there have been many reports on the rates of flux cancellation (in Mx h⁻¹ or equivalent unit) in cancelling magnetic features, the specific rate of flux cancellation (in Mx h⁻¹ Mm⁻¹ or equivalent unit) has been hardly measured until Litvinenko (1999) attempted to explain the rate of flux cancellation using the reconnection model. Moreover, even if it has been well-known that magnetic fluxes of opposite polarities should converge for flux cancellation to occur, not many careful measurements of the converging speed have been done so far.

It may be Litvinenko and Martin (1999) who first measured the specific cancellation rate and the converging speed of a cancelling magnetic feature at the same time. They used a NSO/Kitt Peak daily full-disk magnetogram to determine the initial magnetic flux and the sizes of the cancelling magnetic features, and used Big Bear Solar Observatory magnetograms to determine the cancellation time. As a result, they obtained the specific cancellation rate of 3.5×10^6 G cm s⁻¹ from the observed initial magnetic flux 4×10^{19} Mx, the cancellation time 4 h, and the length along the sheet 7.9 Mm. This value is higher than our values, being about three times ours. They also obtained the converging speed of 0.22 km s⁻¹ from the diameter of the cancelling flux fragments across the sheet 3.2 Mm and the cancellation time. This value is a little smaller than, but not much different from the value we obtained for case A. Note that all the observed converging speeds are in the previously

reported speed range of supergranulation motion (e.g., Wang and Zirin, 1988; Lisle et al., 2000). This supports the idea that the magnetic reconnection in charge of cancelling magnetic features may be driven by the supergranular motion (e.g., Dere, 1994).

In conclusion, compared with Litvinenko and Martin (1999), our measurements produced much smaller specific cancellation rates and somewhat higher converging speeds. The differences may be due to either using different kinds of data, or measuring different cancelling magnetic features, or adopting different methods of data analysis. In any case, it would be interesting to examine our measurements based on the Sweet-Parker type reconnection model as done by Litvinenko and Martin (1999).

4. PHYSICAL IMPLICATIONS

4.1. COMPARISON WITH LITVINENKO'S RECONNECTION MODEL

Litvinenko (1999) assumed an approximate equality of temperatures outside and inside of the current sheet, and obtained the equation for v_i

$$v_i = \left[\frac{\eta B_i}{b\sqrt{4\pi\rho_i}} \right]^{1/2} \left[1 + \frac{B_i^2}{8\pi p_i} \right]^{1/4} \quad (6)$$

for a given magnetic field strength B_i at the inflow region. Here b , the vertical extent (width) of the current sheet, was set equal to the density scale height of the atmosphere Λ . The parameters p_i and ρ_i are the pressure and density of the inflow region. Replacing B_i by the specific rate of flux cancellation r

$$r = v_i B_i, \quad (7)$$

we can obtain a non-linear equation for v_i

$$v_i = \left[\frac{\eta r}{b\sqrt{4\pi\rho_i}} \right]^{1/3} \left[1 + \frac{r^2}{8\pi p_i v_i^2} \right]^{1/6} \quad (8)$$

with a given r .

Litvinenko (1999) argued for the temperature minimum region at height $z \approx 500$ km as the most probable height of magnetic reconnection. At this height, we have, from the model C of Vernazza et al. (1981), $\rho_i = 4.9 \times 10^{-9}$ g cm $^{-3}$, $p_i = 1.3 \times 10^3$ erg cm $^{-3}$ and $\Lambda = 100$ km, and, from the calculation by Kovitya and Cram (1983) $\sigma = 9.9 \times 10^{10}$ s $^{-1}$ and $\eta = 7.2 \times 10^8$ cm 2 s $^{-1}$. Thus, using the observed

value $r = 1.2 \times 10^6 \text{ G cm s}^{-1}$ for case A, we finally obtain $v_i = 0.076 \text{ km s}^{-1}$ from Equation (8). This inflow speed is much smaller than the observed converging speed $v_c = 0.27 \text{ km s}^{-1}$. Why do they so much differ from each other? We examine several possible explanations of the discrepancy below.

4.2. POSSIBLE EXPLANATIONS

4.2.1. *Slowing-down by Flux Pile-up*

We have found that the converging speeds apparently slowed down. But we have indicated that this observed slow-down may not be real, and the speed of magnetic flux transport may be constant down to a distance from the interface of flux cancellation that is spatially well resolved. Nevertheless this result is not fully excluding the possibility that the flux transport might slow down due to the pile-up of magnetic flux in the spatially-unresolved thin layer ($\leq 1000 \text{ km}$) very near to the cancellation interface.

Suppose the observed converging speed v_c is the speed outside the thin layer and the theoretical speed v_i is the speed inside the layer. Then, the condition of flux conservation requires the ratio of the magnetic field strength near the interface B_i to the field strength outside the thin layer B_{ext} to be equal to $v_c/v_i = 3.5$. From Equation (7), we have $B_i = 160 \text{ G}$, and from the 14:23 UT magnetogram in Figure 1, we have $B_{\text{ext}} = \Phi_+/A = 2.0 \times 10^{19} \text{ Mx}/(8 \text{ Mm} \times 4 \text{ Mm}) = 63 \text{ G}$. Finally, we have $B_i/B_{\text{ext}} = 2.5$, a value greater than unity, but a little smaller than v_c/v_i . Therefore, the hypothetical slow-down by flux pile-up can explain a part, if not all, of the discrepancy between v_i and v_c .

4.2.2. *Magnetic Filling Factor*

It has been well-known that magnetic flux in the photosphere usually occupies only a small portion of the spatial resolution element (e.g., Stenflo, 1985; Lin, 1995). An area filling factor α that is much less than unity affects the observational determination of the contact length and the specific rate of flux cancellation in the way

$$L = L_{\text{obs}} \sqrt{\alpha} \quad (9)$$

$$r = r_{\text{obs}} / \sqrt{\alpha}. \quad (10)$$

Suppose most of the flux is concentrated into thin flux tubes with an intrinsic field strength of about 1200 G . Then the filling factor is given by $\alpha = B_{\text{obs}}/B_{\text{true}} = 63/1200 = 0.053$, and the new estimate of the rate of flux cancellation is $r = 1.2 \times 10^6 / \sqrt{0.053} = 5.2 \times 10^6 \text{ G cm s}^{-1}$. Inserting this new value of r into Equation 8 produces $v_i = 0.16$

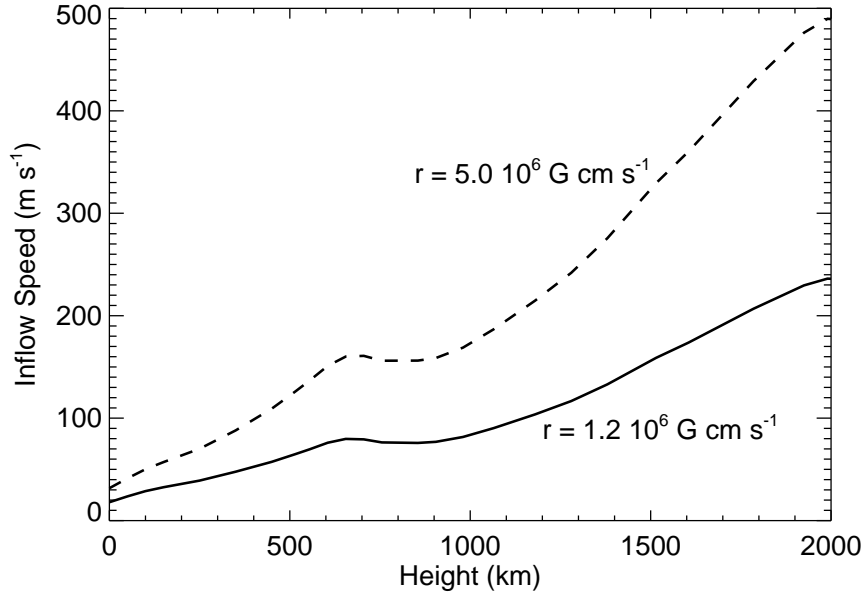


Figure 4. The inflow speed as a function of reconnection height for the prescribed rates of flux cancellation per unit length.

km s^{-1} , a value significantly larger than the previous estimate 0.076 km s^{-1} , but still smaller than $v_c = 0.27 \text{ km s}^{-1}$.

4.2.3. *Low Electric Conductivity*

Another way of explaining the high value of the approaching speed is to use a value of η^* much higher than the calculated value η . Previous studies suggested that the electric conductivity may be very low in the low atmosphere of the Sun. Wang (1993) showed that the calculation of σ near the temperature minimum is very sensitive to the adopted model of atmosphere, and it can be as low as 10^{10} s^{-1} in the Harvard-Smithsonian Reference Atmosphere. Feldman (1993) argued that the electric conductivity in the low atmosphere of the Sun can be as low as 10^9 s^{-1} . Suppose $\sigma = 10^{10} \text{ s}^{-1}$, which corresponds to $\eta^* = 10\eta = 7.2 \times 10^9 \text{ cm}^2 \text{ s}^{-1}$. Then we obtain $v_i = 0.15 \text{ km s}^{-1}$, a value significantly larger than the previous estimate 0.076 km s^{-1} , but still smaller than $v_c = 0.27 \text{ km s}^{-1}$.

4.2.4. *Reconnection at a Higher Level*

If reconnection occurs at a higher level, the inflow speed becomes higher since the density of the inflow region becomes much lower. Figure 4 presents the inflow speed as a function of reconnection height for the

Table II. Physical parameters of magnetic reconnection that were derived from observations and Litvinenko's model.

assumed parameters	Area filling factor α	0.05
	Reconnection height z	500 km
	Electric conductivity σ	$1 \times 10^{10} \text{ s}^{-1}$
	Inflow mass density ρ_i	$4.9 \times 10^{-9} \text{ g cm}^{-3}$
	Inflow pressure p_i	$1.3 \times 10^3 \text{ erg cm}^{-3}$
	Current sheet width b	100 km
derived parameters	True contact length $L = L_{obs}\sqrt{\alpha}$	1.7 Mm
	True specific cancellation rate $r = r_{obs}/\sqrt{\alpha}$	$5.1 \times 10^6 \text{ G cm s}^{-1}$
	Magnetic diffusivity η	$7.1 \times 10^9 \text{ cm}^2 \text{ s}^{-1}$
	Inflow speed v_i	0.27 km s^{-1}
	Inflow field strength B_i	190 G
	Inflow Alfvén speed v_{Ai}	7.5 km s^{-1}
	Inflow plasma beta β_i	0.91
	Reconnection rate $M_i = v_i/v_{Ai}$	0.036
	Lundquist number bv_{Ai}/η	1.1×10^3
	Current sheet thickness a	2.6 km
	Outflow pressure p_o	$2.7 \times 10^3 \text{ erg cm}^{-3}$
	Outflow mass density ρ_o	$1.0 \times 10^{-8} \text{ g cm}^{-3}$
	Outflow speed v_o	5.2 km s^{-1}
	Outflow field strength B_o	4.9 G

prescribed rates of flux cancellation per unit length. The smaller rate is the observed one, and the higher rate is the one taking into account the magnetic filling factor. Note that the VAL-C model parameters and Kubat and Karlicky (1986)'s electric conductivities have been used. The figure shows that the inflow speed at a higher level of, for example, $z \approx 1400 \text{ km}$, is 0.15 km s^{-1} for the observed flux cancellation, and is 0.30 km s^{-1} if a higher rate of flux cancellation taking into account magnetic filling factor is used.

4.2.5. Combined Effect of Low Filling Factor and Low Electric Conductivity

If two of the effects discussed above are combined, it is easy to yield a high value of inflow speed from the reconnection model. For example, with a low filling factor $\alpha = 0.05$ and a small electric conductivity of 10^{10} s^{-1} , the Sweet-Parker magnetic reconnection model based on the observed cancellation rate in example A yields 0.27 km s^{-1} for the

inflow speed of magnetic reconnection occurring at the temperature minimum, which is the same as the observed converging speed.

Table II presents a list of all the physical parameters determined from the magnetic reconnection model. Of our interest is the predicted outflow speed of about 5 km s^{-1} . If the observed outflow is directed upward, it is likely to be manifest as a blue-shift of a strong absorption line such as $\text{H}\alpha$. Recently, Lee et al. (2000) reported the existence of numerous short-lived upflow events in $\text{H}\alpha$ on the Sun with the mean speed of about 5.0 km s^{-1} that is very close to the predicted outflow speed. Therefore, we conjecture that the observed upflow events may be the $\text{H}\alpha$ manifestation of outflow in magnetic reconnection near the temperature minimum.

5. CONCLUSION

We have studied the time evolution of two cancelling magnetic features in detail, and have obtained two kinds of important physical parameters: the specific rate of flux cancellation and the converging speed. Application of the Sweet-Parker type reconnection model has indicated that the observed converging speed is much higher than the theoretical inflow speed. However, there is a good possibility that the discrepancy can be resolved by taking into account one or, more probably, a combination of different kinds of effects such as flux pile-up, magnetic filling factor, lower electric conductivity, and higher reconnection level.

Acknowledgements

This work was supported by the NSF grant: ATM-0086999 and the NASA grants: NAG5-7837, NAG5-9682, NAG5-10894, the 2001 research fund of Chungnam National University, and the BK21 project of the Korean Government.

References

- Chae J., Wang H., Lee C., Goode P. R., and Schuehle U.: 1998, *Astrophys. J.*, **497**, L109.
- Chae J., Qiu J., Wang H., and Goode P. R.: 1999, *Astrophys. J.*, **513**, L75.
- Chae J., Denker C., Spirock T. J., Wang H., and Goode P. R.: 2000, *Solar Phys.*, **195**, 333.
- Chae J., Wang H., Goode P. R., Strous, L., and Yun, H. S.: 2001, *Astrophys. J.*, , in press.

- Dere K. P., Bartoe J.-D. F., Brueckner G. E., Ewing J., and Lund P.: 1991, *J. of Geophys. Res.*, **96**, 9399.
- Dere K. P.: 1994, *Advances in Space Research*, **14**, 13.
- Feldman U.: 1993, *Astrophys. J.*, **411**, 896.
- Harvey, K. L., Jones, H. P., Schrijver, C. J., and Penn, M. J.: 1999, *Solar Phys.*, **190**, 35.
- Hermans L. M., and Martin S. F.: 1986, *Coronal and Prominence Plasmas*, 369.
- Kim J., Yun H. S., Lee S., Chae J., Goode P. R., and Wang H.: 2001, *Astrophys. J.*, **547**, L85.
- Kovitya, P., and Cram, L.: 1983, *Solar Phys.*, **84**, 45.
- Kubat J., and Karlicky M.: 1986, *Bulletin of the Astronomical Institutes of Czechoslovakia*, **37**, 155.
- Lee C., Chae J., and Wang H.: 2000, *Astrophys. J.*, **545**, 1124.
- Lin, H.: 1995, *Solar Phys.*, **446**, 421.
- Lisle J., De Rosa M., Toomre J., 2000, *Solar Phys.*, 197, 21
- Litvinenko, Y.: 1999, *Astrophys. J.* **515**, 435.
- Litvinenko, Y., and Martin S. F.: 1999, *Solar Phys.*, **190**, 45.
- Livi S. H. B., Wang J., and Martin S. F.: 1985, *Australian J. of Physics*, **38**, 855.
- Livi S. H. B., Martin S., Wang H., and Ai G.: 1989, *Solar Phys.*, **121**, 197.
- Martin S. F.: 1986, *Coronal and Prominence Plasmas*, 73.
- Martin, S. F.: 1990, *IAU Symposium*, **138**, 129.
- Martin S. F., Livi S. H. B., and Wang J.: 1985, *Australian J. of Physics*, **38**, 929.
- Stenflo J. O.: 1985, *Solar Phys.*, **100**, 189.
- Sturrock, P. A.: 1999, *Astrophys. J.*, **521**, 451.
- Vernazza, J. E., Avrett, E. H., and Loeser, R.: 1981, *Astrophys. J. Suppl.*, **45**, 635.
- Wang J., 1993, *ASP Conf. Ser.* **46**: *IAU Colloq. 141: The Magnetic and Velocity Fields of Solar Active Regions*, 465.
- Wang J., and Shi Z., 1993, *Solar Phys.*, **143**, 119.
- Wang, J., Shi, Z., and Martin, S. F.: 1996, *Astron. Astrophys.*, **316**, 201.
- Wang H., and Zirin H.: 1988, *Solar Phys.*, **115**, 205.
- Webb, D. F., Martin, S. F., Moses, D., and Harvey, J. W.: 1993, *Solar Phys.*, **144**, 15.
- Zhang, J., Wang, J., Deng, Y., and Wu, D.: 2001, *Astrophys. J.*, **548**, L99.